Chapter 1

Nuclear Physics in Ultra-relativistic Heavy-Ion Collisions

1.1 The Standard Model

The Standard Model describes the fundamental particles of the universe in terms of fermions and bosons. Fermions are particles with half-integer spin, while bosons have integer-spin. This difference in spin has far reaching consequences. Fermions must obey the Pauli Exclusion Principle: only one fermion at a time can occupy a given state. However, multiple bosons can simultaneously occupy a specific state.

Among the fermions are the leptons, neutrinos, and quarks. The leptons consist of the electron, muon, and tau, as well as their anti-particles. The leptons are seemingly fundamental: high energy experiments have yet to observe internal lepton-structure. Neutrinos are weakly interacting particles detected primarily through the precise measuring of missing transverse energy in the products of particle collisions. Quarks are the constituent particles of baryons, which contain three valence quarks, and mesons, which contain two valence quarks. In addition to the valence quarks are the sea quarks, which appear and disappear as quark-antiquark pairs within hadrons. The hadrons are particles made of quarks and gluons.

The behavior of fundamental particles is best described within the framework of quantum field theory (QTF). QFT defines a Lagrangian for fundamental particles. This Lagrangian then predicts the outcome of particle collisions. Different terms in the Lagrangian correspond to the various interactions between particles. The Standard Model Lagrangian can be broken down into four basic terms:

$$\mathscr{L}_{StandardModel} = \mathscr{L}_{QED} + \mathscr{L}_{QCD} + \mathscr{L}_{Higgs} + ... \tag{1.1}$$

The QED and QCD Lagrangians will be the most important in what follows. Feynman rules are derived from the Langrangian. Particularly important for the Feynman rules are the coupling constants for the electromagnetic force and strong-nuclear force.

1.2 Quantum Electrodynamics

Quantum electrodynamics (QED) is a theory of electromagnetic interaction in terms of relativistic quantum field theory. QED addresses three specific processes: photon motion, electron motion, and the emission, or absorption, of a photon by an electron.

The QED coupling decreases with distance, as manifest the Coulomb force being proportional to an inverse-square law.

$$\alpha_{QED}(Q^2) = \frac{\alpha_{em}}{(1 - \frac{\alpha_{em}}{3\pi})\ln(\frac{Q^2}{m^2})} \tag{1.2}$$

1.3 Quantum Chromodynamics

The quarks are a family of fermions that compose the baryons and the mesons. Baryons consist of three quarks in a color neutral state, while mesons consist two quarks in a color neutral state. "Color" in this context refers to the six kinds of strongly-interacting charge available to quarks: red and anti-red, blue and anti-blue, and green and anti-green. Color charge has no relation to optical phenomena, but provides a useful analogy for the stable combinations of quarks. The net color-charge of a baryon or meson is "white".

Unlike QED, the QCD coupling increases with distance. This has the practical consequence of the strong-interactions being stronger in high momentum transfer collisions. The direct results of the running QCD coupling are the dual phenomena of asymptotic freedom and color confinement. At large distances, string tension describes the binding force of the quarks. At short distances,

however, Coulomb-like interactions dominate.

Within the nucleus, a proton can be thought of as a bubble in a vacuum. Debrye screening exerts a pressure on the proton. This pressure is responsible for the size of the proton.

$$\alpha_{QCD}(Q^2) = \alpha_s(Q^2) = \frac{4\pi}{(11 - \frac{2}{3}n_f)\ln(\frac{Q^2}{\Lambda^2_{QCD}})} \tag{1.3}$$

1.4 QCD Experiments

Scattering experiments are the basic tool for exploring the nucleus. The Large Hadron Collider (LHC) is capable of reaching heavy-ion collision energies of up to 7 TeV per nucleon-nucleon. The higher the energy, the more experiments can probe the nuclear phase-space diagram.

At the turn of the century, Ernst Rutherford probed the gold atom by bombarding a gold sheet with alpha-particles (helium nuclei). The angular distribution of the scattered alpha-particles demonstrates that the mass of the atom is concentrated in a small volume, i.e, the atom is mostly empty space.

Momentum transferred, expressed as Q^2, is an important quantity for characterizing QCD measurements.

In addition to Q^2, Bjorken-x, also known as Bjorken-scaling is necessary to describe the nuclear phase space. Bjorken-x represents the momentum fraction of partons.

1.5 Deep Inelastic Scattering

Deep inelastic scattering commonly refers to the scattering of a leptons off hadrons. Experiments at HERA focused on electron-proton collisions. In these collisions, the electron was used as a source of photons and neutrinos. When these particles scatter off the proton, the dependence of the collision cross section, on momentum transfer and scattering angle of the source electron, reflects the structure of the proton. These experiments provided the first evidence of two phenomena: the parton model and Bjorken-scaling.

The parton model, first proposed by Richard Feynman, posits that hadrons in general, and nucleons in specific, are made of more fundamental constituent particles which may or may not be the quarks implied by the SU(3) symmetry. In addition to the quarks, the partons also include any field quanta associated with nuclear forces. In time, these field quanta are dubbed "gluons".

"Scaling" is an interpretation of the data from deep inelastic scattering. First proposed by James Bjorken, scaling is reflected in the incoherence of photon-proton interactions at photon energies above 1 GeV/c.

Soft processes compose the low momentum transfer, typically gluon-gluon interactions during a collision.

1.6 Ultra-peripheral Heavy-Ion Collisions

Similar to the Rutherford experiment, in heavy-ion collisions the scattered particles carry information about the internal structure of the nucleus.

The Rutherford experiment has the three components that still characterize high-energy nuclear experiments: a probe, a medium, and a signal. Alpha particles probe the medium of the gold atom, and the angular distribution of scattered alpha particles signals the internal structure of the atom.

Ultra-peripheral collisions occur at impact parameters greater than the sum of the heavy-ion radii. In these collisions, hadronic interactions are strongly suppressed while photonuclear activity is enhanced proportional to the square of the nuclear charge. The electromagnetic field of an incoming heavy-ion, from the perspective of a target, is equivalent to a flux of virtual photons.

Gluons are the particle exchanged in strong interactions. However, gluons themselves carry color charge. By analogy, photons transmit the electromagnetic force, but do not themselves have an electric charge.

When a quark is scattered from a nucleus, the strong interaction gathers potential energy until the threshold for quark production is passed, at which point an anti-quark is generated to screen the ejected quark.

QCD factorisation describes the diffractive-photoproduction dijet cross-section as the convolu-

tion of the partonic cross-section with the diffractive parton distributions. However, factorisation only describes H1 data if the resolved-photon contribution is suppressed.

The photoproduction cross-section is proportional to the gluon distribution.

At low momentum transfer, photons interact electromagnetically, i.e. directly, with partons.

High energy photons possess a hadronic structure.

Chapter 2

Diffractive Dijet Photoproduction

2.1 Factorization

Diffractive dijet photoproduction is not describable in perturbative QCD. For coherent processes the photon energy is small, and therefore the wavelength is large compared to the size of the nucleus. At these large distances, there isn't a hard scale, and so perturbation calculations cannot be done. Gluon splitting interactions dominate the low Bjorken-x partons. QCD collinear factorization describes these soft interactions via the convolution of parton cross sections, taken from perturbative QCD, and diffractive parton distribution functions, taken from experiment.

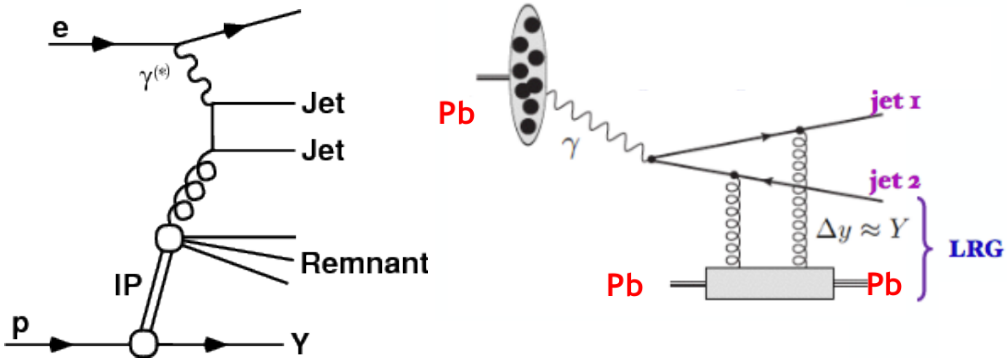

In electron-hadron collisions, diffractive photoproduction is characterized by the presence of a large rapidity gap in the final state and an intact nucleus. The Feynman diagram of electroproduction in lepton-hadron collisions is similar to that of photoproduction in ultraperipheral collisions. The diffractive dijet cross section is expressed by the convolution of partonic cross sections $d\hat{\sigma}$ and diffractive PDFs $f^D_{i/p}$.

$$d\sigma(ep \to e+2jets+X^{'}+p) = \sum_i \int dt \int dx_{\mathbb{P}} \int dz_{\mathbb{P}} d\hat{\sigma}_{ei\to 2jets}(\hat{s},\mu_R^2,\mu_F^2) \times f_{i/p}^D(z_{\mathbb{P}},\mu_F^2,x_{\mathbb{P}},t) \tag{2.1}$$

In proton vertex factorisation, the dependence on $x_{\mathbb{P}}$ and $|t|$ is factored into a dependence on μ_F^2 and $z_{\mathbb{P}}$.

$$f_{i/p}^D(z_{\mathbb{P}},\mu_F^2,x_{\mathbb{P}},t) = f_{\mathbb{P}/p}(x_{\mathbb{P}},t) f_{i/\mathbb{P}}(z_{\mathbb{P}},\mu_F^2) + n_{\mathbb{R}} f_{\mathbb{R}/p}(x_{\mathbb{P}},t) f_{i/\mathbb{R}}(z_{\mathbb{P}},\mu_F^2) \tag{2.2}$$

Lepton-hadron collisions were performed at DESY and measured by the H1 and HERA experiments. These experiments reported a value for the total diffractive photoproduction cross section that is double that predicted by QCD collinear factorization. Diffractive events were selected for using rapidity gaps or the presence of leading protons in the very forward proton spectrometer (VFPS).

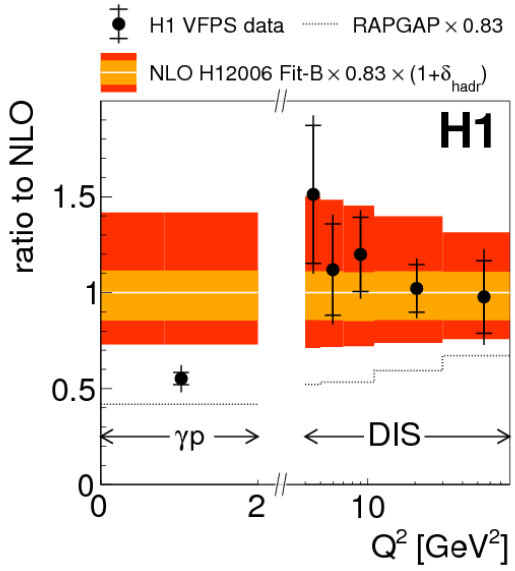

H1 used the Very Forward Proton Spectrometer (VFPS) to trigger on low Q^2 protons. The VFPS consists of two Roman Pots located 218 m and 222 m from the H1 interaction-point in the forward direction. The VFPS can detect protons scattered at very low transverse momentum, corresponding to $0.008 < x_P < 0.028$ and $|t| < 0.6$. Each of the Roman Pots contains layers

of scintillating fibers, which are covered by a layer of scintillator tiles. The fibers readout to photomultipliers, and the tiles both shield from radiation and trigger on protons. The track effiency of VFPS is a remarkable 96%, and the background contamination is kept at 1% , making the detector excellent for studying diffractive events.

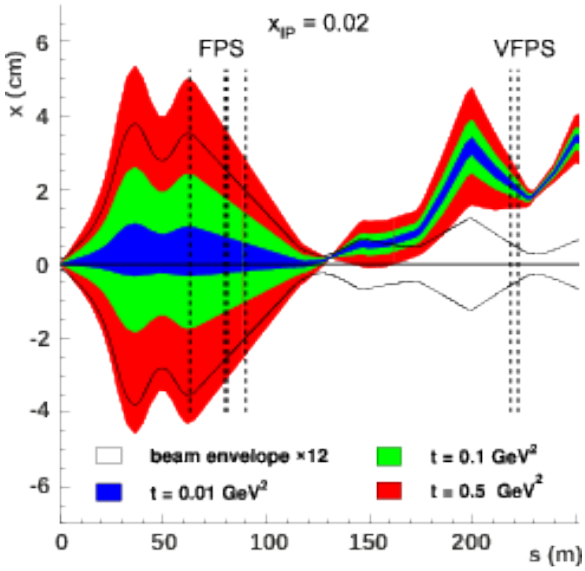

The H1 data was compared to predictions based on NLO-QCD convoluted with diffractive parton distribution functions (DPDFs) from HERA inclusive diffractive deep-inelastic scattering (DDIS) data. For diffractive pp collisions the high transverse momentum jets yield a hard scale for perturbative QCD.

2.2 Wigner Distribution

The quantum field theory lagrangian of the strong interaction is relatively simple, but because of confinement and asymptotic freedom the hadronic bound states are too complex for an analytic solution. Furthermore, collider experiment data requires a quantitative interpretation to be useful. The gap between QCD and heavy-ion data is bridged using the parton model, which considers hadrons as composed of quarks and gluons. Parton density functions (PDFs) model the longitudinal momentum distribution of the partons. PDFs are supplemented by transverse momentum

distributions (TMDs) and generalized parton distributions (GPDs). In addition to transverse momentum, GPDs describe the transverse spatial distribution. TMDs and GPDs are derived from the final state particles of a collision. Markus Diehl maps the relationship between various distribution functions in figure X.

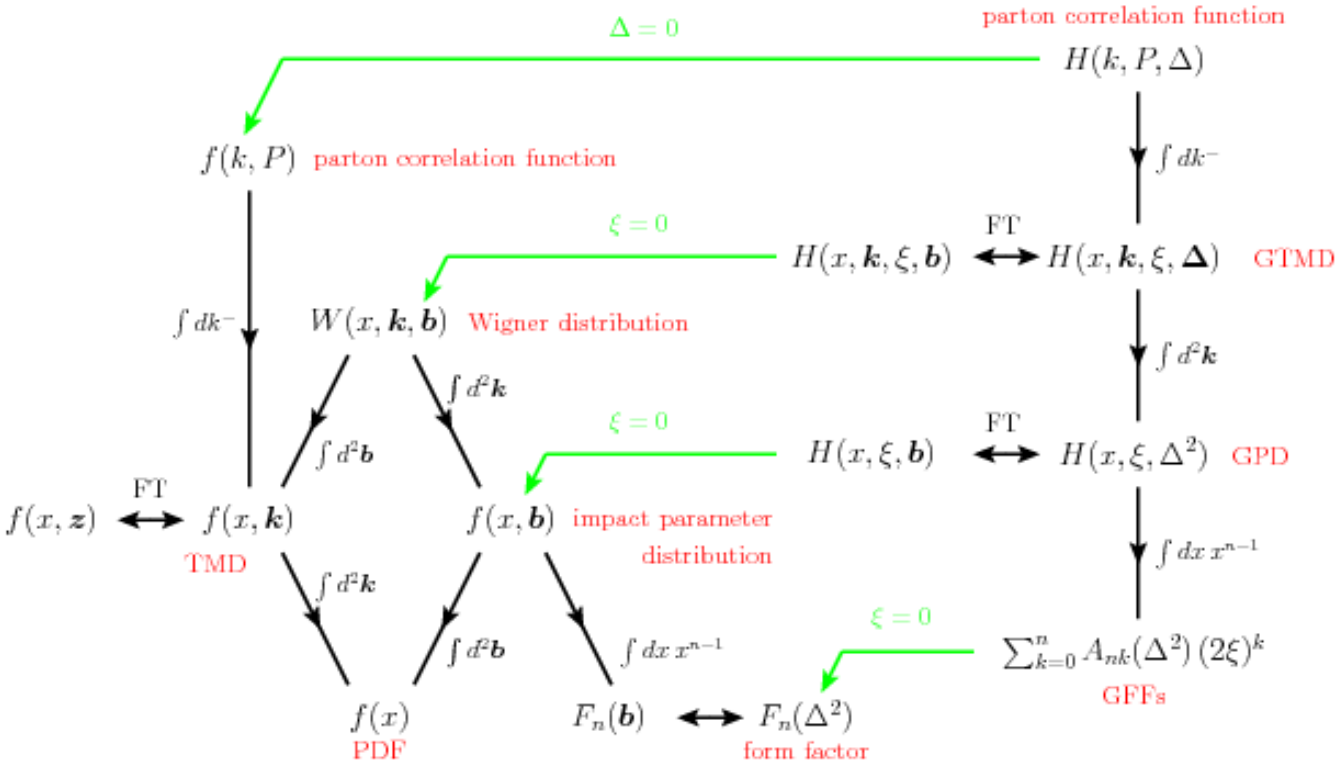

TMDs and GPDs manifest non-perturbative QCD effects. The Wigner distribution, at this scale, reflects the relationship between the position and momentum of partons.

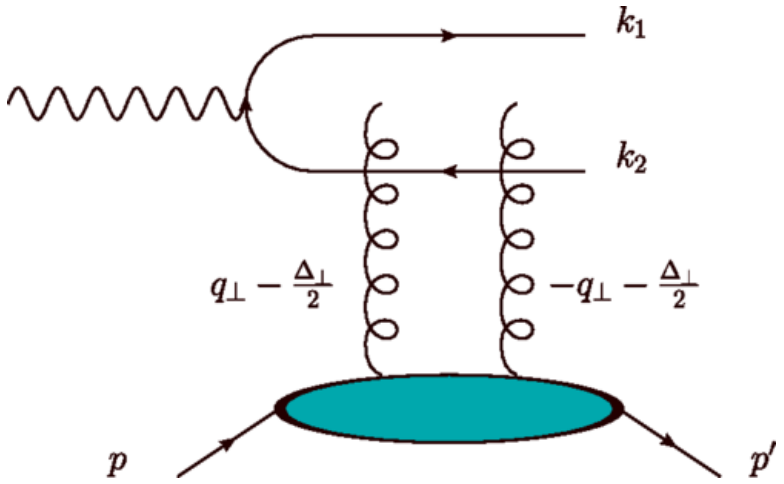

Yoshitaka Hatta uses the dipole framework to show that the azimuthal angular correlations of coherent dijets are generated by the underlying gluon Wigner distribution. Furthermore, these correlations are consistent with predictions based on standard collinear factorization.

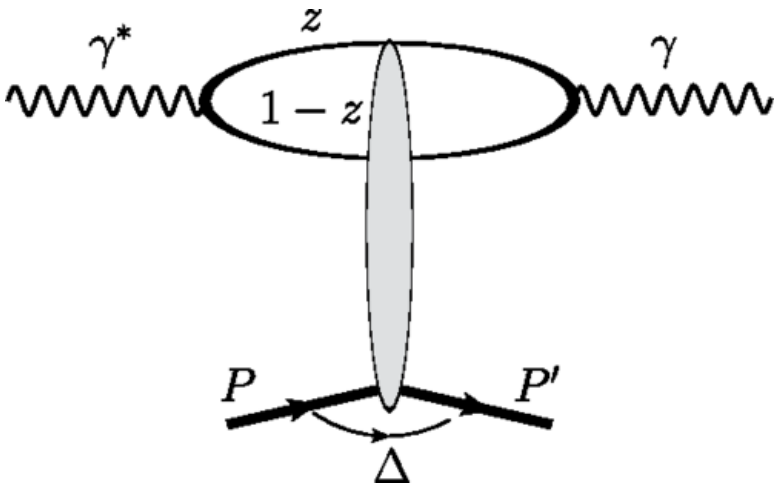

Chapter 3

The Experiment

3.1 Large Hadron Collider

The Large Hadron Collider (LHC) has a radius of approximately 27 kilometers. As of this writing, it is the largest machine ever constructed. The initial purpose of the LHC was to discover the Higgs boson, but it is capable of investigating a variety of other physics phenomena, such as dark matter, extra-dimensions, and heavy-ion physics.

The beams are accelerated along a circular path using radio frequency cavities, gaining energy with each revolution. LHC is a hadron collider, meaning it is designed to collide particles made of quarks and gluons. The proton-proton, proton-Pb, and Pb-Pb collision energies are the largest ever probed experimentally. The LHC is a circular collider.

Heavy-ion collisions at LHC produce strongly interacting nuclear matter. The temperature and density of this matter is comparable to the state of the universe only a few milliseconds after the Big Bang.

3.2 Compact Muon Solenoid

The Compact Muon Solenoid (CMS) is a general-purpose particle detector located at Point-5 of the LHC. CMS was designed to precisely measure the momentum of muons. The titular superconducting solenoid magnet was designed to generate a 4 Tesla field, but operates at 3.8 T to increase longevity. This field is homogeneous and parallel to the beam line close to the interaction point. The momentum of a muon is measured from how it deflects when moving through the magnetic

field. Altogether, CMS weighs approximately 12,500 metric tons, with a diameter of 14.6 m and a length of 21.6 meters.

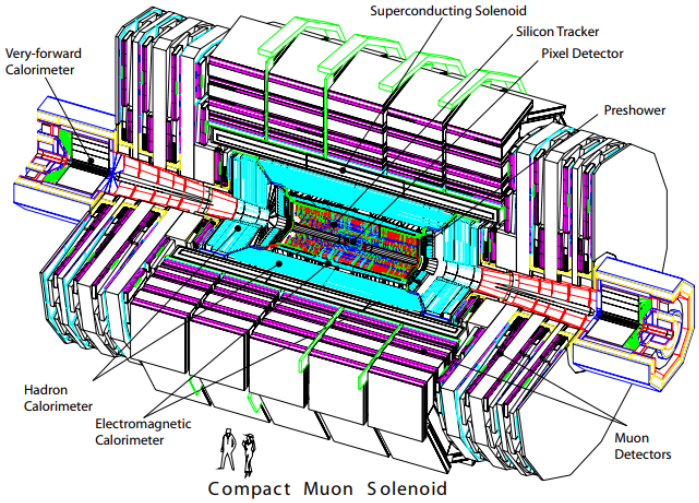

Within the solenoid volume are a silicon pixel and strip tracker, a lead tungsten crystal electromagnetic calorimeter (ECAL), and a brass and scintillator hadron calorimeter (HCAL), each composed of a barrel and two endcap sections.

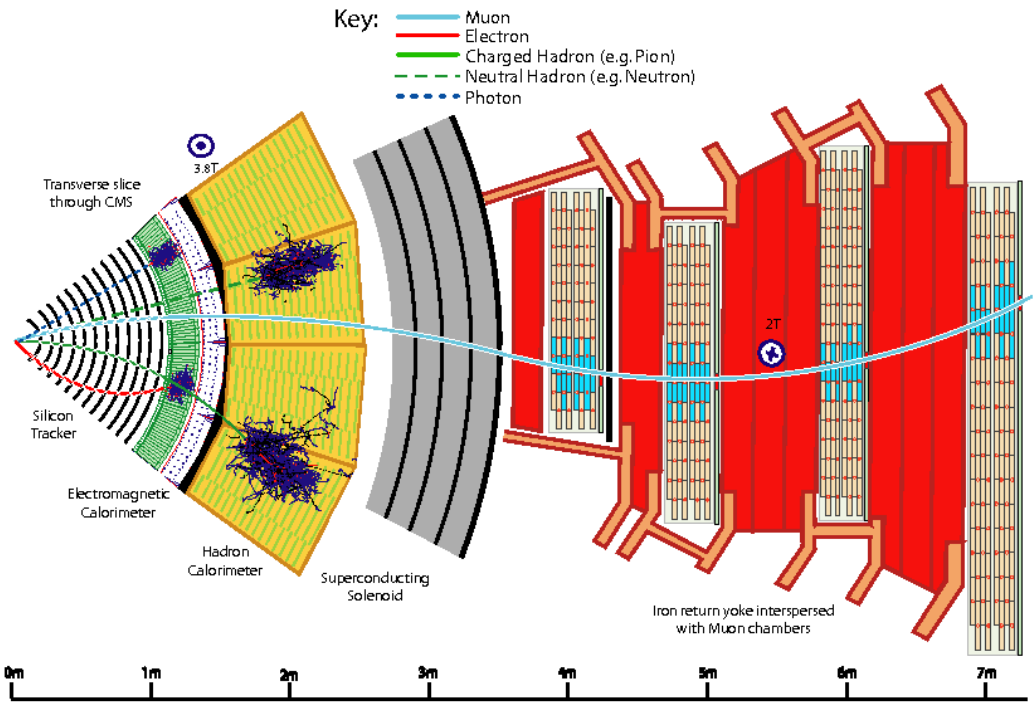

3.2.1 Tracker

The tracker measures the momentum of charged particles via their trajectory through a homogenous magnetic field. The tracker consists of two units, the pixel tracker and the strip tracker, both of which are made of silicon. A charged particle causes an electrical signal when passing through a silicon pixel or silicon microstrip. CMS reconstructs these electrical signals, taken at specific points of position and time, into tracks. These tracks are accurate to 10 micrometers. The tracker is meant to have a particle pass all the way through it, with only minimal effect particle's trajectory.

The tracker system is designed for high granularity and fast readout, such that each trajectory can be associated with its corresponding bunch crossing. The tracker is resilient enough to withstand the high flux of particles accompanying every bunch crossing; at design luminosity of $10^34cm^-2s^-1$, some 1000 particles will traverse the tracker every 25 ns. However, the mass of the tracker is minimal enough to suppress multiple scattering, off its material, that would distort particle trajectories. These design constraints – resistance and transparency – are satisfied silicon. The tracker has approximately $200m^2$ of silicon surface, making it the largest silicon detector ever constructed.

3.2.1.1 Pixel Tracker

Every silicon-pixel has a corresponding readout chip. The readout chips are soldered through the bump-bonding method. The readout chip amplifies signals from the pixel. The pixel tracker is precise enough to distinguish the vertices of tracks originating from short-lived particles, such as bottomonia. The innermost elements of the pixel tracker come within 4.4 cms of the CMS interaction point. The pixel tracker covers a pseudorapidity range of $|\eta| < 2.5$ with some 66×10^6 separate pixels.

3.2.1.2 Strip Tracker

Outside the pixel tracker are the layers of the strip tracker. They function similar to the components of the pixel tracker, except the strip tracker consists of thin silicon plates. The strip tracker itself

can be broken down into four components: the inner barrel layer, the inner endcaps, the outer barrel layer, and the outer endcaps. In total, these layers contain some 9.3×10^6 strips.

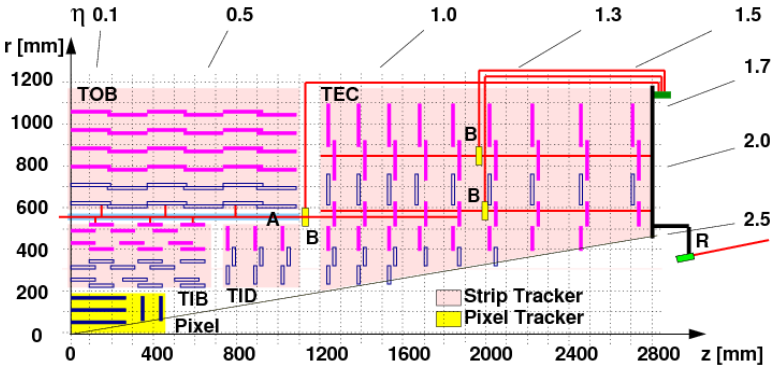

3.2.2 Electromagnetic Calorimeter

The Electromagnetic Calorimeter (ECAL) is the dedicated CMS calorimeter for detecting electrons and photons. The calorimeter is comprised of lead tungstate ($PbWO_4$) crystals arranged in cylinder about the beam, including two endcaps. The granularity of these crystals gives the ECAL excellent energy resolution, angular resolution, and spatial resolution; for example, the ECAL has the resolution suitable for the decay of the Higgs boson into two photons. The ECAL is both hermetic and homogenous.

The data readout is fast enough that CMS can trigger off signals in the ECAL. It takes about 25 ns for an ECAL hit to scintillate 80 percent of its lights, putting the calorimeter's rate on the same scale as the bunch crossing. Scintillation in the crystals activates photodetectors that transmit information to the L1 trigger. In the barrel these photodectors are avalanche photodiodes (APDs). The endcaps use vacuum phototriodes (VPTs).

3.2.3 Hadronic Calorimeter

The Hadronic Calorimeter (HCAL) is the next layer outside the tracker. HCAL is a sampling calorimeter, meaning that it absorbs particles and measures their energyy and momentum via scintillation. HCAL has such a large acceptance that it can indirectly observe non-interacting particles

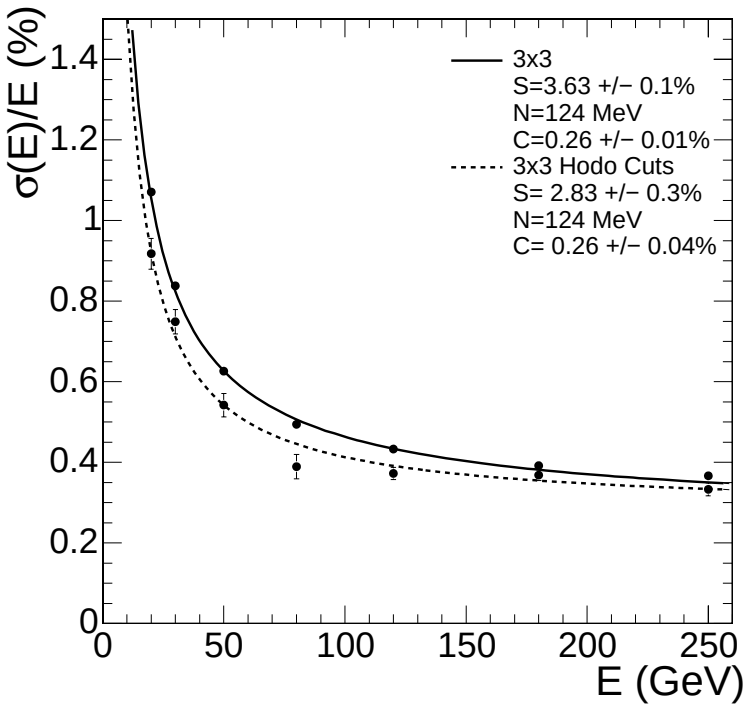

such as neutrinos. The HCAL is designed to be hermetic, so that imbalances of momentum and energy can be precisely measured.

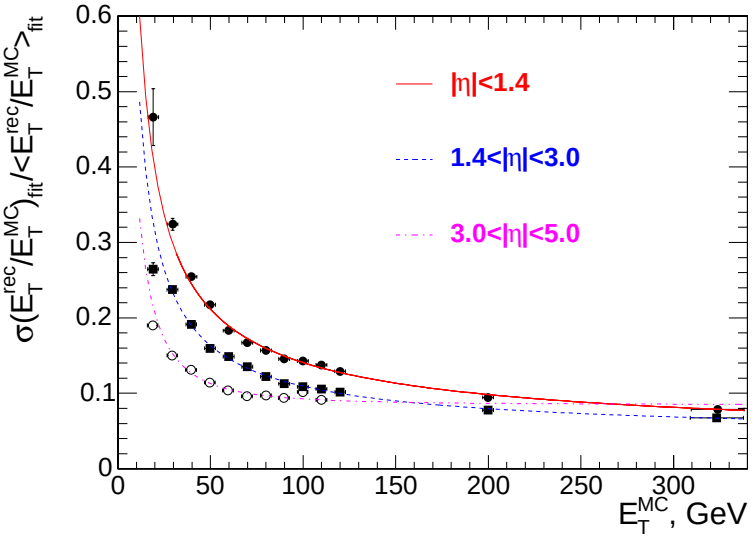

3.2.3.1 Hadronic Forward Calorimeters

The Hadronic Forward Calorimeters (HF) absorbs the greatest portion of energy from collisions. As such it is designed for maximum radiative resistance. Hits in the HF are used to measure the instantaneous luminosity of CMS. The HF encompasses ($3.0 < |\eta| < 5.2$) and complements the coverage provided by the barrel and endcap detectors.

3.2.4 Muon Detector

The outermost layer of CMS consists of the muon detectors. Muons are particles nearly identical to electrons, except for their mass, which exceeds that of the electron by some two orders of magnitude. High mass particles, like the Higgs boson, often decay into a final state containing muons. The muon detector not only identifies muons, but also measures their momentum. The muon detector has readout fast enough for triggering on muons.

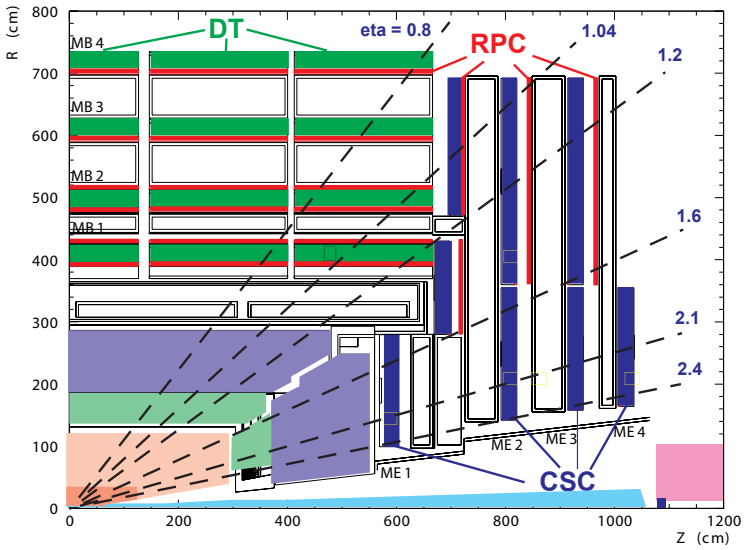

3.2.5 Zero Degree Calorimeter

The zero degree calorimeters are both sides of CMS, approximately 140 meters from the interaction point. Each ZDC consists of two independent systems: an electromagnetic calorimeter, for detecting very forward photons, and a hadronic calorimeter, for detecting neutrons. Because these

neutrons result from the dissociation of nuclei, the ZDC can measure the centrality of heavy-ion collisions. Hadrons in the forward region have energy on the TeV scale, so the ZDC's hadronic calorimeter is made of thick tungsten plates. For a UPC process, the photon emitting nucleus is most likely to remain intact; therefore, ZDC data can the photon direction of a process, and by extension it's energy.

3.2.6 Particle Flow Algorithm

Raw data from the sub-detectors is combined, for data analysis, by the particle-flow (PF) algorithm. The PF takes the data about tracks in the tracker and energy deposits in the calorimeter, and uses them to reconstruct physics-related data objects, like jets, and to identify specific particles, such as photons and muons. The PF also identifies missing energy and momentum for use in neutrino studies. These data objects are stored in a format similar to that of conventional MC event generators. CMS gains significant jet reconstruction efficiency via the PF. At low transverse momentum, PF reconstructs jets at nearly twice the resolution of HCAL and ECAL. This increase in efficiency comes from the PF integrating in track data with the calorimeter tower data.

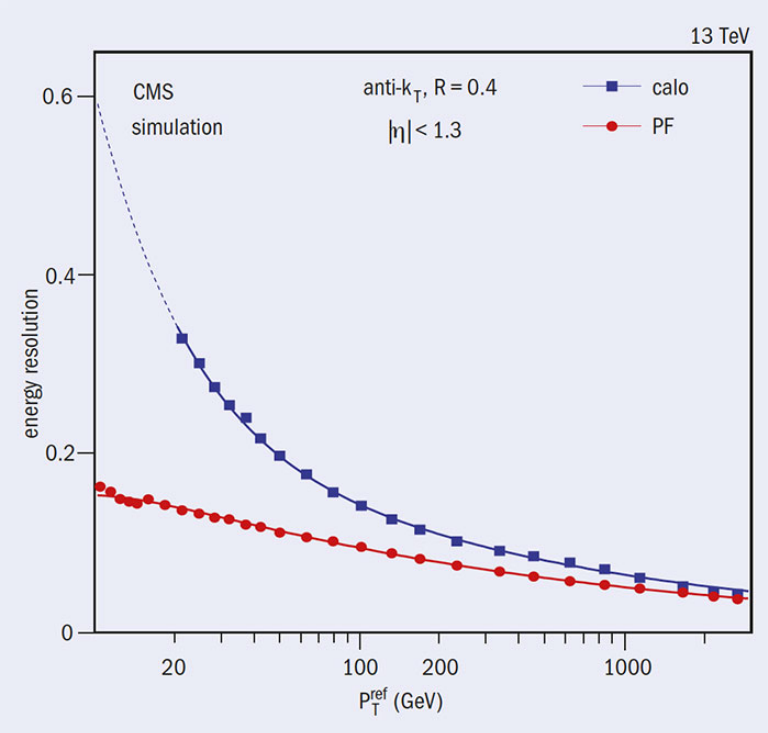

3.2.7 Luminosity

One of the most important quantities measured by CMS is luminosity. Luminosity is necessary to convert the number of events detected, for a given channel, into a collision cross-section. Collision cross-sections are among the primary observables predicted by theoretical physics, specifically quantum field theory. For particle physics, the collision cross-section of a process is typically measured through the relation:

$$\sigma = \frac{R}{L} \tag{3.1}$$

Where σ is the cross-section, R is the rate at which the process occurs per collision, and L is the luminosity.

3.2.7.1 van de Meer Scanning

The luminometers of CMS produce signals proportional to the instantanteous luminosity of the LHC beam. However, these signals need to be properly calibrated with respect to a known visible cross-section for each luminometer. This calibration is accomplished via Van de Meer scanning. The opposing beams of LHC are moved back and forth in the transverse plane. During the scan, the detector response is measured as a function of beam displacement. The beam widths are calculated from Gaussian fits to the detector response. The visible cross-section of the luminometer in question is then derived from the width of the beams, and acts as the calibration of the detector response.

3.2.8 Triggering

CMS uses a two-tiered triggering system. The first tier, the L1 trigger, is hardware based. The second tier, the high-level trigger (HLT), is software based. The L1 trigger recieves raw data from the calorimeters and the muon detectors; this determines when the tracker will readout data. The raw data from the tracker, calorimeters, and muon detectors is then passed on to a computer farm

running the HLT menu. The HLT then performs a simplistic reconstruction of the raw data into physics objects useful for analysis: jets, tracks, and identifiable particles. If an event passes the HLT, the raw data is permanently stored in preparation for a more complex reconstruction.

The 2015 UPC triggers were for low multiplicity events and low transverse momentum events.

For this analysis, the L1 trigger applies two selections. First, the L1 checks that at least one of the HF is empty. This is the most important part of the trigger in so far as it suppressed the hadronic contamination of the dataset. Then, if there is at least 5 GeV of energy deposited in the ECAL, the event passes to the HLT.

Low multiplicity events are difficult to distinguish from background. To compensate, the HLT in turn requires that there be at least once reconstructed track from the pixel tracker, to make sure that there are particles that will be reconstructed by the complete tracker. Only the pixel tracker is used for these HLTs to increase the speed of reconstruction while decreasing needed computer cycles.